Build Simul (2020) 13: 931–941
https://doi.org/10.1007/s12273-020-0631-4

Effects of ambient pressure on smoke movement patterns in vertical shafts in tunnel fires with natural ventilation systems

Guanfeng Yan[1,2], Mingnian Wang[1,2], Li Yu[1,2] (✉), Ruyu Duan[1,2], Pengxi Xia[1,2]

1. Key Laboratory of Transportation Tunnel Engineering, Ministry of Education, Southwest Jiaotong University, Chengdu 610031, China
2. School of Civil Engineering, Southwest Jiaotong University, Chengdu 610031, China

Abstract

Smoke exhaust is of vital importance for life safety and structural safety in a tunnel fire. The smoke movement pattern could affect smoke exhaust efficiency, so it is necessary to determine the patterns in shafts in tunnel fires with natural ventilation systems. However, previous studies have focused on this problem at standard atmospheric conditions, but the ambient pressure, which could have an effect on smoke movement characteristics and temperature distribution, decreases in high-altitude areas. First, theoretical analysis is carried out to find that the smoke velocity is higher under reduced pressure due to lower heat loss. In addition, a set of numerical simulations based on Fire Dynamics Simulator (FDS) is conducted to investigate the effects of ambient pressures on smoke movement patterns in vertical shafts in tunnel fires with natural ventilation systems. The results show that the critical Richard number deceases under reduced ambient pressure, and the higher smoke temperature and velocity caused by lower ambient pressure are the reasons for the decrease in critical Ri. We hope that our work can provide a design reference for tunnel natural ventilation system design in high-altitude areas.

Keywords

ambient pressure,
vertical shafts,
plug-holing,
boundary-layer separation,
high-altitude area,
natural ventilation

Article History

Received: 24 August 2019
Revised: 21 February 2020
Accepted: 29 February 2020

1 Introduction

With the development of the economy of China, the process of urbanization is accelerating with a large number of people from villages migrating to cities. As the population becomes increasingly larger, traffic congestion becomes worse and there is limited available space in urban areas, so exploiting the space underground could be an efficient solution to these problems. As a result, many urban road tunnels are being constructed in China. However, it is easy for the buoyancy-driven smoke to accumulate under the ceiling in a tunnel when a fire breaks out since the tunnel is a narrow and confined structure, unlike other engineering structures (Zhao and He 2017; Meng et al. 2018;), which leads to poor ventilation capacity. As a result, it is of vital importance to discharge the toxic gas induced by fire because the data show that most casualties result from smoke instead of the fire (Alarie 2002).

Generally, there are two methods for removing toxic gas from vehicle emissions and fire-induced smoke, namely, natural ventilation and mechanical ventilation. Mechanical ventilation requires a great deal of money during the initial construction stage, and during the operation period, ventilation equipment consumes a large amount of energy and requires maintenance, which makes mechanical ventilation costly. In comparison with mechanical ventilation, natural ventilation is an economical method for enhancing the environment in tunnels. Extensive works have been carried out to investigate the temperature distribution and smoke exhaust efficiency of shafts (Wang et al. 2016b; Liu et al. 2019; Zhao et al. 2019).

Wang et al. (2009) explored the fire characteristics in a tunnel with roof openings under natural ventilation system conditions through full-scale experiments and compared the experimental results with numerical simulations. They found that rood openings are reliable for discharging the smoke generated by a fire source since most smoke flowed directly out of the openings, and smoke may backflow and sink along with smoke temperature attenuation, which could pose a threat to stranded people. Ji et al. (2012) conducted a set of reduced-scale experiments to explore the smoke

E-mail: yuli_1026@swjtu.edu.cn

movement pattern in vertical shafts in a tunnel fire with various shaft heights. The results showed that when the shaft height is small, the boundary-layer separation is apparent, and plug-holing could occur with an increase in shaft height. Both of these phenomena could lower the efficiency in smoke exhaust of natural ventilation systems. As a result, Ji et al. (2012) proposed a concept of critical height between boundary-layer separation and plug-holing and used a modified Richard number for determination. In addition, Fan et al. (2013) also argued that a strong mixing process was witnessed around the exhaust vent between the smoke layer and cold air layer, which could decrease the smoke exhaust efficiency with an amount of air charged out through the exhaust vent. Ji et al. (2013) also explored the influence of shaft geometry on the smoke exhaust process in urban tunnels with natural ventilation and found that a shaft with a large cross-section could be divided into several small shafts to improve exhaust efficiency, avoiding the plug-holing phenomenon. Kashef et al. (2013) and Yuan et al. (2015) presented formulas to predict the temperature distribution in tunnel fires with natural ventilation based on theoretical analysis and reduced-scale experiments. They divided the tunnel into two sections, the fire and non-fire sections, and determined that temperature decay was an exponential equation function. Zhong et al. (2013) investigated the influence of longitudinal wind on smoke flow characteristics of a road tunnel fire with a vertical shaft and found that a critical velocity existed, leading to a better smoke exhaust effect. There have been some other studies researching the smoke exhaust efficiency of natural ventilation considering the geometry parameters of vertical shaft (Ji et al. 2014; Zhu et al. 2015; Baek et al. 2017a; Baek et al. 2017b; Takeuchi et al. 2018; Xie et al. 2018; Zhang et al. 2018), fire source factors (Fan et al. 2018a), tunnel sloping (Tanaka et al. 2016; Zhong et al. 2016;Li et al. 2017), ambient wind (Fan et al. 2017; Tanaka et al. 2017; Fan et al. 2018b) and shaft inclination (Yao et al. 2019b). A method featuring solid screens below the shafts (Cong et al. 2017; Zhou et al. 2019) was proposed to increase the efficiency of exhausting the smoke by accumulating fire-induced smoke and reducing the effects of plug-holing. Moreover, many scholars have explored the temperature distribution (Wang et al. 2015; He et al. 2017; Takeuchi et al. 2017; Tanaka et al. 2017; Fan et al. 2018b; Guo et al. 2019; Liu et al. 2019) and back-layer length (Wang et al. 2016a; Wang et al. 2016b; Yao et al. 2016; Wan et al. 2019; Yao et al. 2019a; Zhao et al. 2019) in a tunnel fire with shafts.

Although many works have been conducted by numerous researchers (Harish and Venkatasubbaiah 2014; Ji et al. 2016), previous works have focused on natural ventilation in a tunnel fire at standard atmospheric pressure, while ambient pressure decreases with increasing altitude (Wang et al. 2019), and some papers have shown that ambient pressure could affect smoke movement characteristics and temperature distribution (Tang et al. 2014; Ji et al. 2017; Yan et al. 2017; Ji et al. 2018). It has been known that the longitudinal smoke temperature could be higher under lower ambient pressure due to lower heat loss (Ji et al. 2017) and smoke temperature is the factor that most influences the smoke velocity (Kim 1998). In previous studies (Jie et al. 2010; He et al. 2018), researchers concluded that smoke velocity around the exhaust vent or shaft affects the smoke movement pattern or occurrence of plug-holing to a large extent. Therefore, ambient pressure may influence the smoke movement pattern in a vertical shaft in a tunnel fire with a natural ventilation system (Yan et al. 2020). However, few studies have investigated the effects of ambient pressure on smoke movement patterns in vertical shafts in a tunnel fire.

In this paper, theoretical analysis shows that the smoke velocity in the shaft is higher under reduced ambient pressure due to higher smoke temperatures. In addition, a set of numerical simulations are conducted to investigate the effects of ambient pressure on the smoke movement pattern in a vertical shaft in a tunnel fire. We found that the critical *Ri* is smaller under reduced ambient pressure due to higher smoke velocity caused by higher smoke temperature. We hope that our work can provide a reference for ventilation design in tunnels in high-altitude areas.

2 Theoretical analysis

2.1 Smoke movement patterns in vertical shafts

In previous papers (Ji et al. 2012), there are two modes for the smoke movement pattern in a vertical shaft in a tunnel, i.e., boundary-layer separation and plug-holing, as shown in Figure 1. The ratio of vertical buoyancy force and horizontal inertia force of smoke without exhaust dominates the pattern. The horizontal inertia force is related to the height of the shaft. For boundary-layer separation, the height of the shaft is small, and the buoyancy-driven smoke flow will separate from the upstream wall of the shaft (the side near the fire source is considered to be the upstream) while passing the shaft bottom and entering the shaft. As the height of the vertical shaft increases, the horizontal inertia force rises, and the pattern of smoke movement converts to plug-holing. As this time, some cold air is directly drawn into the shaft, mixing with the smoke due to the strong vertical buoyancy force.

2.2 Smoke thickness calculation method

The smoke thickness is an important factor since the life of stranded people could be endangered if the smoke height is

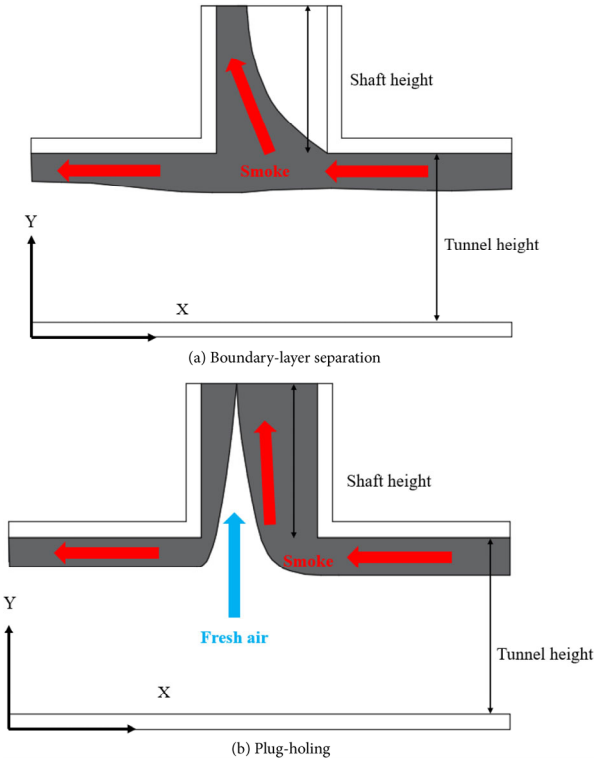

Fig. 1 Smoke movement pattern in the vertical shaft

lower because the concentration of toxic gas is higher, and the visibility is lower in this case. There are several methods for calculating smoke height, such as the N-percentage rule (Cooper 1982) and integral ratio method (He et al. 1998). The N-percentage rule is a convenient method for obtaining smoke thickness, but it is subjective for a user to select an N-value. Therefore, a new method is proposed to acquire the smoke height by calculating the integral ratio of the hot smoke layer and cold air layer based on the theory of smoke temperature stratification (Yang et al. 2010).

The integral ratio of the upper smoke layer is:

$$r_u = \frac{1}{(H - H_{int})^2} \int_{H_{int}}^{H} T(z)\mathrm{d}z \int_{H_{int}}^{H} \frac{1}{T(z)}\mathrm{d}z \tag{1}$$

The integral ratio of the lower air layer is:

$$r_l = \frac{1}{H_{int}^{\ 2}} \int_{0}^{H_{int}} T(z)\mathrm{d}z \int_{0}^{H_{int}} \frac{1}{T(z)}\mathrm{d}z \tag{2}$$

The sum of the integral ratio is

$$R_t = r_u + r_l \tag{3}$$

where H represents the tunnel height, H_{int} is the interface between the air and smoke, and $T(z)$ is the vertical temperature distribution of tunnel cross-section. The actual interface is determined when the R_t comes to the minimum value.

In this paper, the integral ratio method is used to calculate smoke height to remove the flaw of subjective judgment.

2.3 Criterion for plug-holing and boundary-layer separation in vertical shafts

In Ji's work (Ji et al. 2012), the Froude number criterion (Hurley 1995) is not suitable for the condition in a tunnel, and a new criterion of a modified Richard number to determine the pattern of smoke movement in a vertical shaft is introduced. The pattern is affected by the ratio of vertical buoyancy force and horizontal inertia force. The vertical buoyancy force (Ji et al. 2012) is given by:

$$F_v = \Delta\rho g h A \tag{4}$$

The horizontal inertia force without smoke exhaust is shown below:

$$F_h = \rho_{s0} v^2 dw \tag{5}$$

The modified Richard number is given by:

$$Ri = \frac{\Delta\rho g h A}{\rho_{s0} v^2 dw} \tag{6}$$

where $\Delta\rho$ is the density difference between smoke and air under the shaft without ventilation, g is the gravity acceleration, h is the shaft height, w is the shaft width, A is the shaft area, ρ_{s0} is the smoke density under the shaft without smoke exhaust, d is the smoke thickness without smoke exhaust, and v is the velocity below the shaft when there is no ventilation. It should be noted that the parameters under a shaft without ventilation reflect cases without a shaft.

The smoke velocity in the vent is the factor that most influences the smoke movement pattern. In this paper, a theoretical analysis of the effects of ambient pressure on smoke velocity is carried out. Figure 2 shows schematics of the smoke exhaust in a tunnel fire with a vertical shaft.

Based on the energy conversation law and the Bernoulli equation, we can obtain the following:

$$(\rho_0 - \rho_s) g h = \frac{1}{2}\rho_s v_s^2 + H_W \tag{7}$$

where ρ_0 is the ambient air density, ρ_s is the smoke density, v_s is the smoke velocity in the shaft opening, and H_W is the pressure loss. The H_W is given by:

$$H_W = \frac{1}{2}\xi_{in}\rho_s v_s^2 + \frac{1}{2}\xi_{out}\rho_s v_s^2 + \frac{1}{2}\frac{\lambda h}{D_{shaft}}\rho_s v_s^2 \tag{8}$$

where ξ_{in} and ξ_{out} are the local pressure loss coefficients at the inlet and outlet of the shaft, λ is the friction coefficient,

Fig. 2 Schematics of the smoke exhaust in a tunnel fire with a vertical shaft

which is related to the relative roughness of the tunnel shaft wall and Reynold number, h is the height of the shaft, D_{shaft} is the hydraulic diameter of the shaft. Ambient pressure barely affects ξ_{in}, ξ_{out} and λ, which are influenced by the geometric parameters of the shaft (Cong et al. 2017).

Combining Eqs. (7) and (8), we obtain:

$$v_s = \sqrt{\left(\frac{\rho_0}{\rho_s} - 1\right)\frac{2gh}{\left(\xi_{in} + \xi_{out} + \frac{\lambda h}{D_{shaft}}\right)}} \tag{9}$$

In addition, the following equation can be obtained based on the ideal gas equation:

$$\frac{\rho_0}{\rho_s} = \frac{T_s}{T_0} \tag{10}$$

In previous studies (Ji et al. 2017; Ji et al. 2018), we concluded that: the temperature of smoke is higher under reduced ambient pressure. Therefore, we can conclude that smoke velocity v_s is higher in the vertical shaft under reduced ambient pressure, which can make it easier for plug-holing to occur (Ji et al. 2010). Therefore, it is necessary to investigate the Ri under various ambient pressures.

3 Numerical modelling

3.1 Fire scenarios

Due to the rapid development of computational techniques, some efficient tools such as the Fire Dynamics Simulator (FDS) developed by the US National Institute of Standard and Technology can help researchers analyse the temperature field and velocity in fire-induced environments (McGrattan and Forney 2017). FDS can solve a series of Navier-Stokes equations to investigate the behaviour of low-speed and thermal-driven flows and has been widely adopted in studying smoke movement and temperature distribution in a tunnel fire. Extensive studies have been conducted based on FDS, and the accuracy of the numerical simulations has been validated by both full-scale and reduced-scale model experiments and theoretical analysis, which proves the reliability of numerical simulations based on FDS.

In comparison with FDS 5, the latest version of FDS (version 6) featuring many advances in hydrodynamics, turbulence models and scalar transport scheme (McGrattan and Forney 2017) contributing to obtaining a more accurate resolution of thermal-driven flows is selected in this paper.

A full-scale tunnel that is 200 m long with a cross-section of 10.8 m wide and 7.2 m high is constructed in the FDS (see Figure 3). The fire source is 90 m away from the right opening of the tunnel, as shown in Figure 3. The vertical shaft is at a distance of 20 m from the fire source, and the area of the shaft cross-section is 9 m^2 with both width and length 3 m. The height of the shaft is adjustable since it can change the smoke movement pattern in the vertical shaft (Ji et al. 2012).

The materials of the tunnel ceiling, sidewalls and floor are set as "CONCRETE" according to engineering practice in China. Both tunnel openings are defined as "OPEN". The heat release rate (HRR) ranges from 5 MW which reflects the car fire to 30 MW representing the truck fire. In China, the highest road tunnel is the Changlashan Tunnel, which is at an altitude of 4,500 m with an ambient pressure of approximately 58 kPa. As a result, the ambient pressure in this work is from 60 kPa to 100 kPa. The opening of the shaft is also set as "OPEN", which indicates natural ventilation, and the height of the shaft ranges from 0 m to 5 m at an interval of 0.5 m. The ambient temperature is set to 20 °C. The summary of all simulated cases is listed in Table 1.

The vertical and longitudinal temperatures beneath the shaft are usually recorded to explore the smoke movement pattern in the shaft in previous studies (Fan et al. 2013; Tanaka et al. 2016). Therefore, in this study, a series of vertical

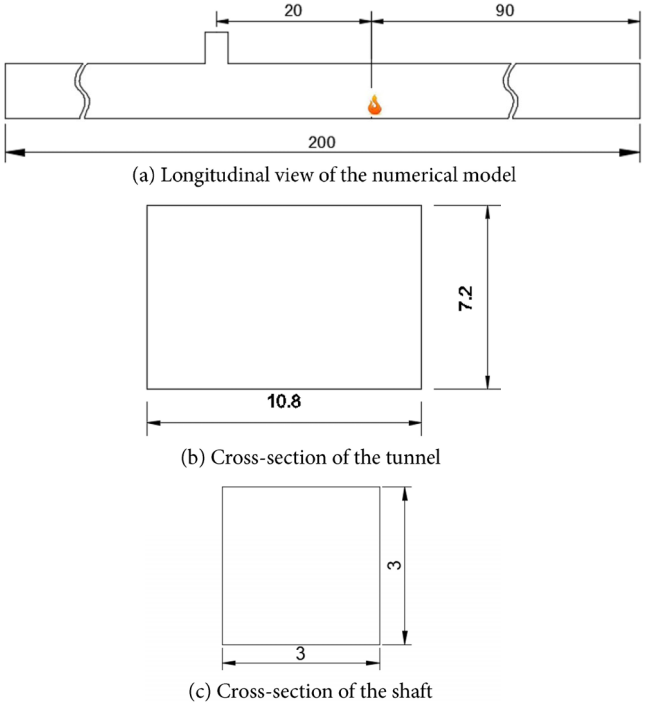

(a) Longitudinal view of the numerical model

(b) Cross-section of the tunnel

(c) Cross-section of the shaft

Fig. 3 Schematic view of the numerical model (unit: m)

Table 1 Summary of all tests

No.	Heat release rate (MW)	Ambient pressure (kPa)	Shaft height (m)
1–33	5	100,80,60	0–5
34–66	15	100,80,60	0–5
67–99	30	100,80,60	0–5

Note: the interval of shaft height is 0.5 m.

thermocouples are just under the shaft to reflect the smoke layer temperature and thickness variation (see Figure 4) and the interval is 0.4 m with the highest thermocouple 0.2 m under the bottom of the vertical shaft. In addition, there are some longitudinal temperature sensors that are 0.2 m under the shaft and at a longitudinal interval of 0.5 m to measure the smoke temperature under the vertical shaft to determine the smoke movement pattern in the shaft (Takeuchi et al. 2017) as shown in Figure 4.

3.2 Grid sensitivity analysis

The accuracy of the numerical study relies on grid quality (Mou et al. 2017; Zhao and He 2017; Meng et al. 2018). In the user's guide of the FDS, the criterion for grid resolution is the ratio of the fire characteristics diameter D^* to the grid size δx.The fire characteristic diameter D^* is defined as:

$$D^* = \left(\frac{\dot{Q}}{\rho_0 c_p T_0 \sqrt{g}}\right)^{2/5} \tag{11}$$

where $\dot{Q}$ is the heat release rate of the fire source, ρ_0 is the ambient density, c_p is the specific heat capacity, T_0 is the temperature of the ambient environment, and g is the gravity

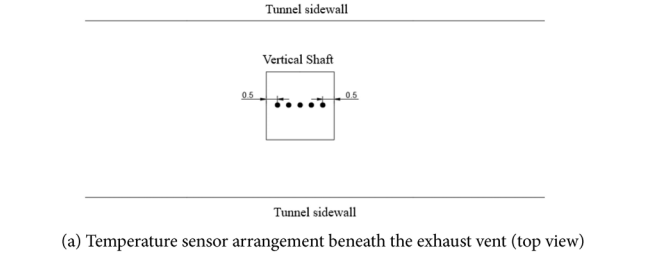

(a) Temperature sensor arrangement beneath the exhaust vent (top view)

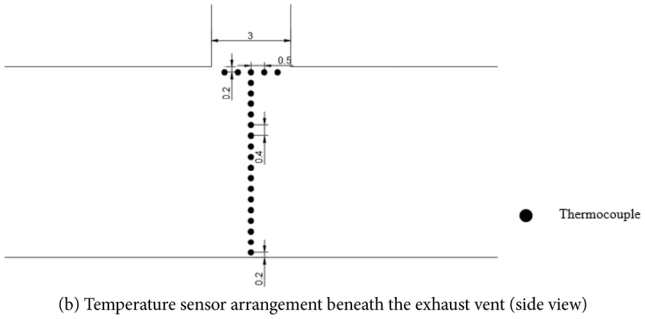

(b) Temperature sensor arrangement beneath the exhaust vent (side view)

Fig. 4 Temperature sensor arrangement beneath the exhaust vent (unit: m)

acceleration. To obtain the proper grid size, a grid sensitivity analysis is carried out and the vertical temperature distributions of the cross-section 35 m away from the fire source when the HRR is 5 MW with various grid sizes in the longitudinal, transverse and vertical dimensions are shown in Figure 5. It is easy to determine that the accuracy is satisfied when the gird size is 0.167 m, and the total time consumed by calculation increases dramatically with grid sizes larger than 0.167 m. As a result, 0.167 m is adopted in this paper, which corresponds with previous studies (Fan et al. 2017; Ji et al. 2017; Fan et al. 2018b; Ji et al. 2018).

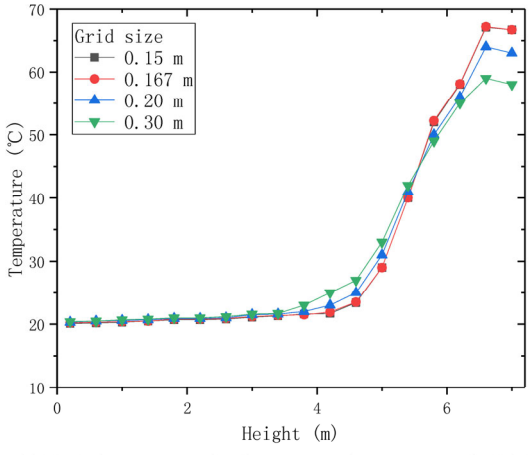

(a) Vertical temperature distributions at ambient pressure of 100 kPa

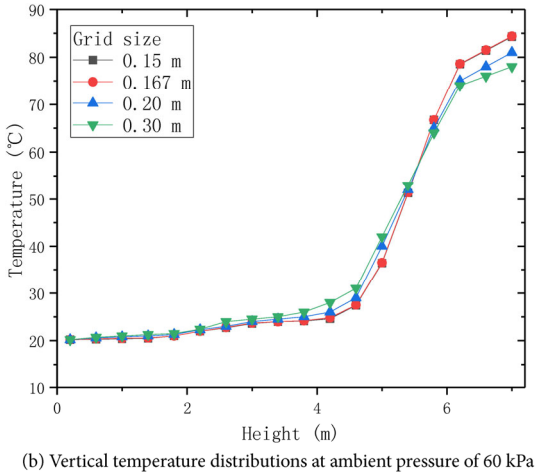

(b) Vertical temperature distributions at ambient pressure of 60 kPa

Fig. 5 Vertical temperature distributions at a distance of 35 m from the fire source with various grid sizes under ambient pressures when the HRR is 5 MW

4 Results and discussions

4.1 Smoke flow pattern in vertical shafts

In a previous study (Takeuchi et al. 2017), the results of longitudinal temperature sensors were adopted to determine the smoke movement pattern. For boundary-layer separation, the temperature under the shaft is uniform, and the smoke

thickness beneath the shaft is not zero. Additionally, the temperature under the shaft varies since the sunken area appears due to the large amount of fresh air drawn out of the shaft directly when plug-holing occurs and at the same time, the smoke thickness decreases to zero.

When the shaft height is small, the smoke movement pattern in the shaft shows boundary-layer separation, while plug-holing occurs when the shaft height reaches a certain height (Ji et al. 2012). When the shaft is 1 m high, the smoke movement shows boundary-layer separation for 30 MW at an ambient pressure of 100 kPa, and the results of longitudinal temperature sensors are shown in Figure 6. We can see that the temperature of the measuring point deceases with increasing distance between the sensor and the fire source, which is located on the right side of the shaft for two reasons: heat loss to the surroundings (Gong et al. 2016) and some heat and smoke is exhausted by the vertical shaft. However, the temperature distribution can be considered to be uniform.

However, the shaft increases to 5 m high, plug-holing appears for 30 MW at an ambient pressure of 100 kPa, and the results of longitudinal temperature sensors are shown in Figure 7. To distinguish the difference of two cases, the upper and lower bounds are set to be the same in Figure 6 and Figure 7. We can conclude that the temperatures of several sensors near the fire source are higher, while those where no smoke exists are lower and close to the ambient temperature. In this case, the sunken area under the shaft appears since a large amount of fresh air is exhausted directly from the vertical shaft.

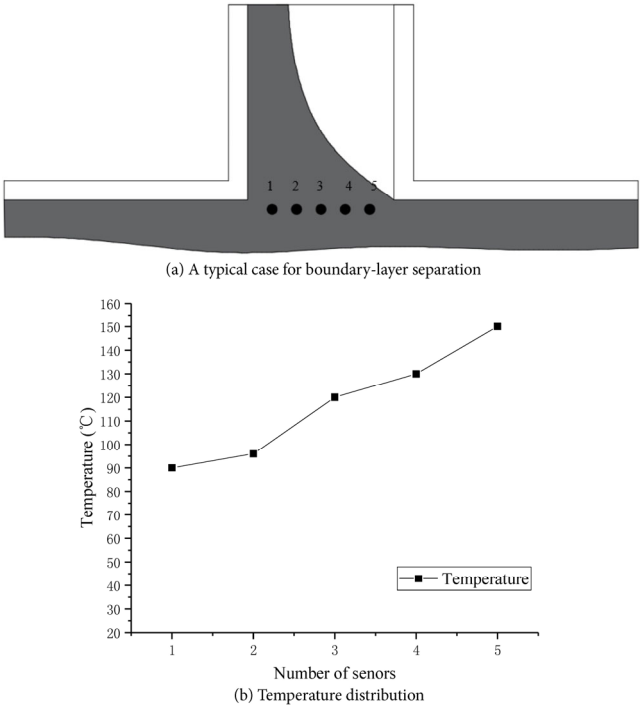

(a) A typical case for boundary-layer separation

(b) Temperature distribution

Fig. 6 A typical case for boundary-layer separation

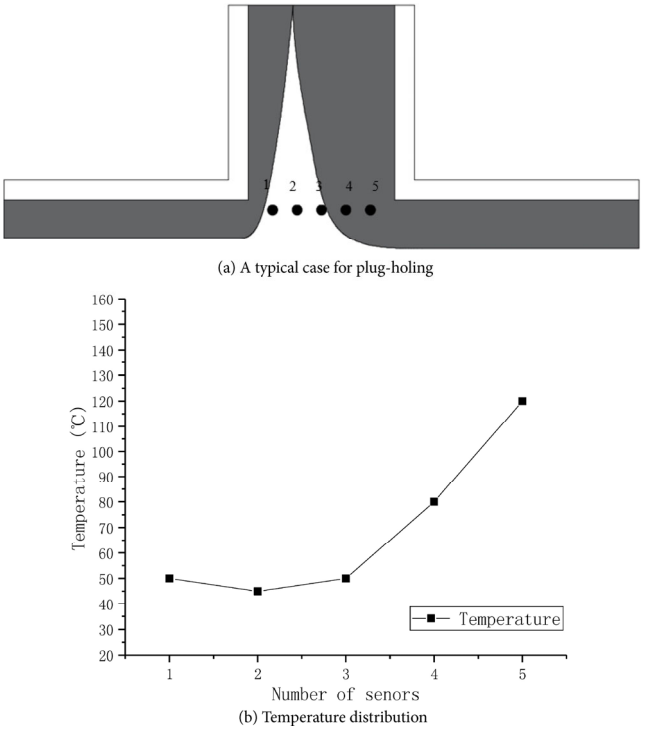

(a) A typical case for plug-holing

(b) Temperature distribution

Fig. 7 A typical case for plug-holing

As a result, we can determine the smoke movement pattern in the shaft by analysing the longitudinal temperature distribution since there is a notable difference between the two cases. The results of all cases are listed in Table 2. We can see that the boundary-layer separation dominates for low shaft height while plug-holing occurs when the height of the shaft reaches a certain value, which increases with an increasing heat release rate and this conclusion applies to all cases under various ambient pressures.

Table 2 Smoke movement pattern in all cases

	HRR								
	100 kPa			80 kPa			60 kPa		
Height (m)	5 MW	15 MW	30 MW	5 MW	15 MW	30 MW	5 MW	15 MW	30 MW
0.5	B	B	B	B	B	B	B	B	B
1	B	B	B	B	B	B	B	B	B
1.5	P	B	B	P	B	B	P	B	B
2	P	P	B	P	P	B	P	P	B
2.5	P	P	P	P	P	P	P	P	B
3	P	P	P	P	P	P	P	P	P
3.5	P	P	P	P	P	P	P	P	P
4	P	P	P	P	P	P	P	P	P
4.5	P	P	P	P	P	P	P	P	P
5	P	P	P	P	P	P	P	P	P

Note: 'B' represents boundary-layer separation; (2) 'P' represents plug-holing.

4.2 The vertical smoke temperature

The vertical smoke temperature is an important factor in determining the pattern of smoke thickness since the smoke temperature can decrease to a low value when plug-holing occurs due to a large amount of fresh cold air being directly drawn out of the shaft.

Figure 8 shows the variation in vertical smoke temperature under the shaft with varying heat release rates and ambient pressures. We can determine that when the shaft height increases, the vertical smoke temperature decreases sharply, but when plug-holing occurs, the smoke temperature decreases slowly and remains approximately stable, which corresponds with Section 4.1 and the previous study (Ji et al. 2012). The ambient pressure and heat release rate do not change the law, but a higher heat release rate could increase the critical value of shaft height.

It should be noted that although plug-holing occurs and a large amount of fresh cold air is drawn directly out of the shaft, the temperature of the measuring point under the shaft does not decrease to the ambient pressure due to the heat transfer and radiation from smoke (Gong et al. 2016). In addition, the vertical smoke temperature under the shaft is higher under reduced ambient pressure because of lower heat loss, which corresponds with previous studies (Ji et al. 2017; Ji et al. 2018).

4.3 The smoke thickness

When plug-holing occurs, the thickness of the smoke layer will decrease to zero, so the smoke thickness could determine the occurrence of plug-holing. As a result, it is necessary to explore the variation in smoke thickness when the height of the shaft increases.

Figure 9 displays the variation in smoke thickness under varying ambient pressures and heat release rates. We can conclude that the result of smoke thickness corresponds with that of the vertical temperature. The patterns of variation in smoke thickness under different heat release rates and ambient pressures are similar. When the shaft height is low and boundary-layer separation dominates, the smoke height decreases. However, after the height of the shaft reaches a certain value, the smoke thickness will remain stable and is nearly zero since plug-holing occurs, and fresh air is exhausted

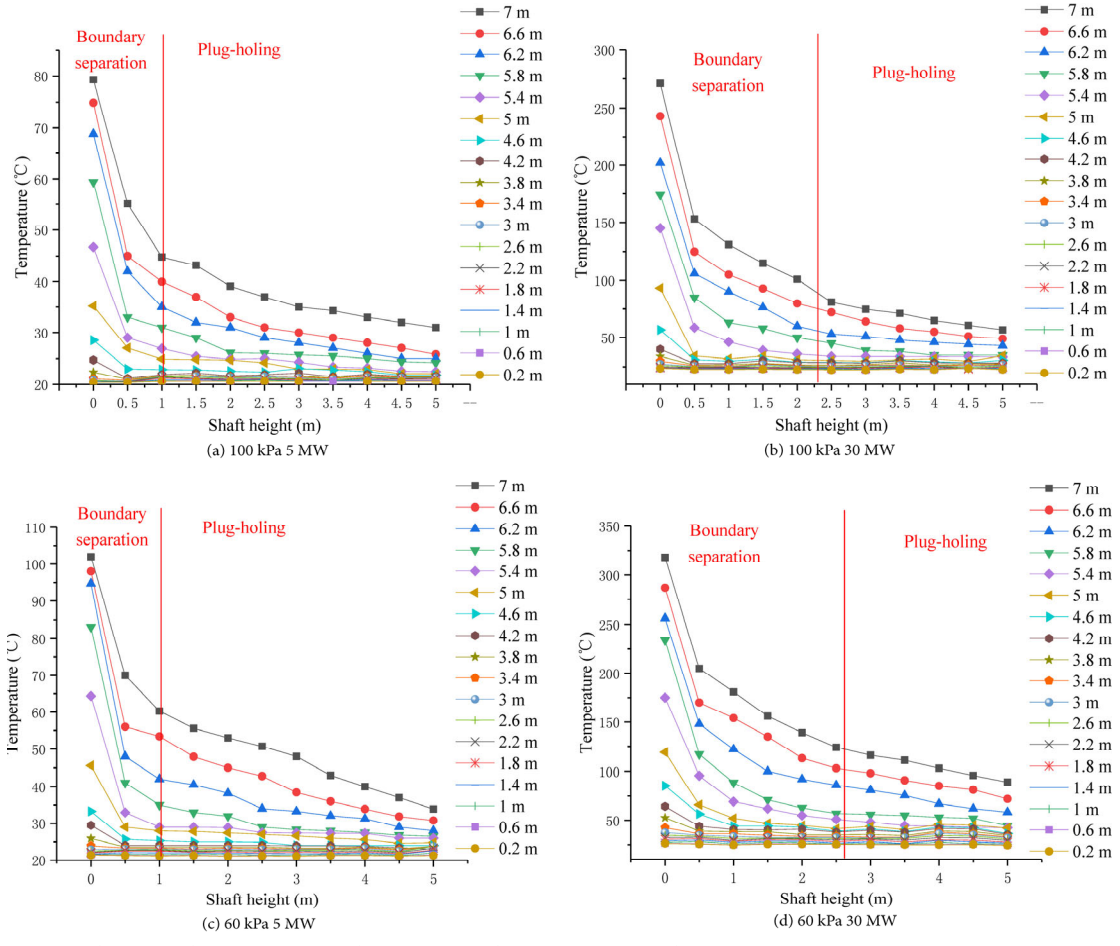

Fig. 8 Variation in the vertical temperature under varying ambient pressures and HRRs

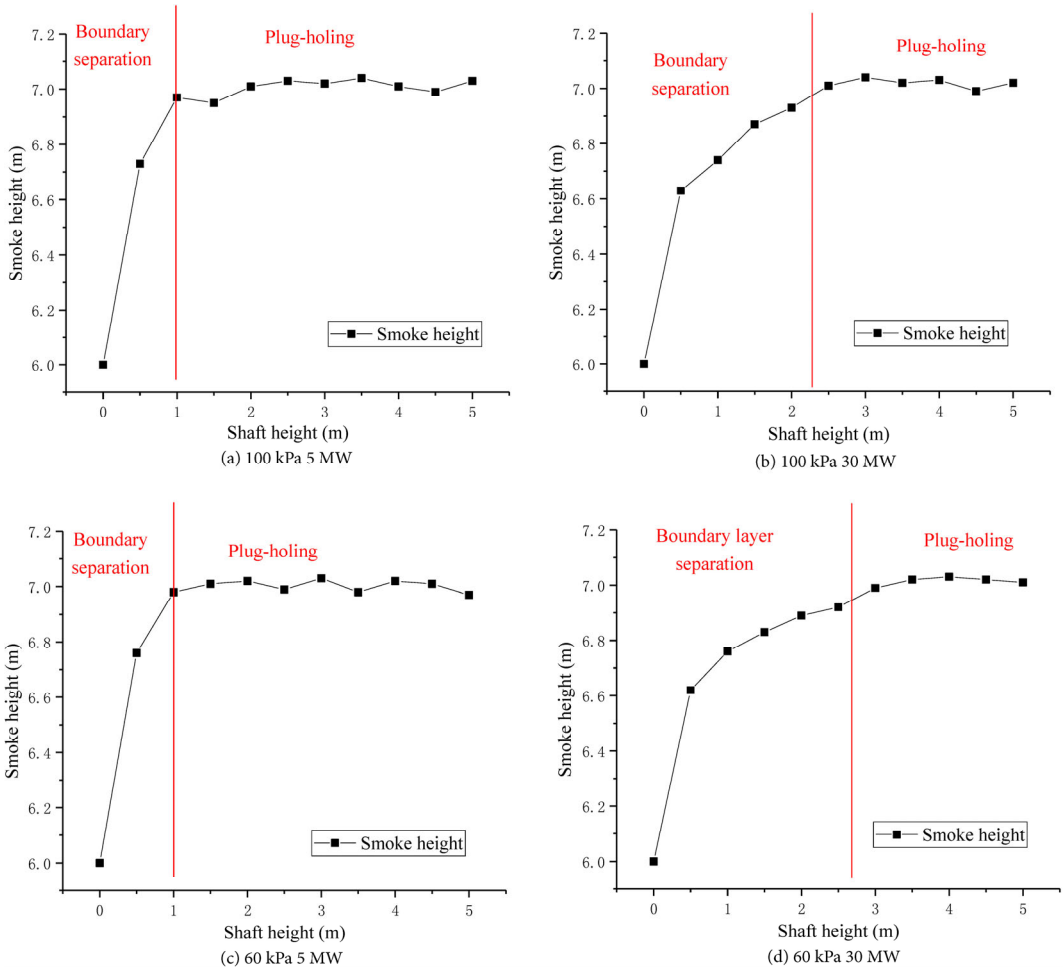

Fig. 9 Variation in smoke thickness under varying heat release rates and ambient pressures

directly out of the shaft. A higher heat release rate increases the critical shaft height, which corresponds with a previous study (Ji et al. 2012) and Section 4.2 in this paper.

4.4 The criterion for smoke movement patterns under various ambient pressures

A previous study (Ji et al. 2012) showed that the dominant driving force of natural ventilation in a tunnel fire is the stack effect which is caused by the density difference between the hot smoke and cold fresh air. The difference in density makes smoke move upward by buoyancy. Ji et al. (2012) presented the Richard number to determine the smoke movement pattern at standard atmospheric pressure. When *Ri* is larger than 1.4, plug-holing occurs. Otherwise, boundary-layer separation dominates in the vertical shaft. However, the critical *Ri* under reduced ambient pressure is not clear.

According to Eq. (6), we can deduce that there are two factors influencing the smoke movement pattern in the shaft: vertical buoyancy force and horizontal inertia force. The parameters of the smoke layer under the exhaust vent without exhausting are listed in Table 3. Table 3 shows that a higher heat release rate indicates a higher smoke temperature and velocity, representing a higher inertia force. Reduced ambient pressure also increases the smoke temperature and velocity due to lower heat loss because of

Table 3 Parameters of the smoke layer under the exhaust vent without exhausting

Ambient pressure	HRR	Ambient temperature (K)	Smoke temperature (K)	Smoke thickness (m)	Smoke velocity ($m \cdot s^{-1}$)
100 kPa	5 MW	293	351	1.2	2.0
	15 MW	293	428	1.2	3.5
	30 MW	293	543	1.2	4.5
80 kPa	5 MW	293	364	1.2	2.2
	15 MW	293	450	1.2	3.8
	30 MW	293	568	1.2	4.8
60 kPa	5 MW	293	375	1.2	2.4
	15 MW	293	479	1.2	4
	30 MW	293	591	1.2	5.4

lower air density (Ji et al. 2017; Ji et al. 2018). In addition, HRR and ambient pressure barely change the smoke thickness, which corresponds with previous studies (Ji et al. 2012; Oka et al. 2016; Jiang et al. 2018).

Figure 10 shows the Richard number with varying ambient pressures and HRRs. According to Table 2, we can obtain the critical *Ri* of all cases. At standard atmospheric pressure, the critical *Ri* is 1.4 which corresponds with a previous study (Ji et al. 2012). In addition, reduced ambient pressure decreases the critical *Ri*, such as critical *Ri* is 1.2 under an ambient pressure of 60 kPa. This conclusion that lower ambient pressure leads to a lower Richard number corresponds with Section 2.3 since smoke in the tunnel shaft moves faster because of higher smoke temperature due to lower heat loss under reduced ambient pressure.

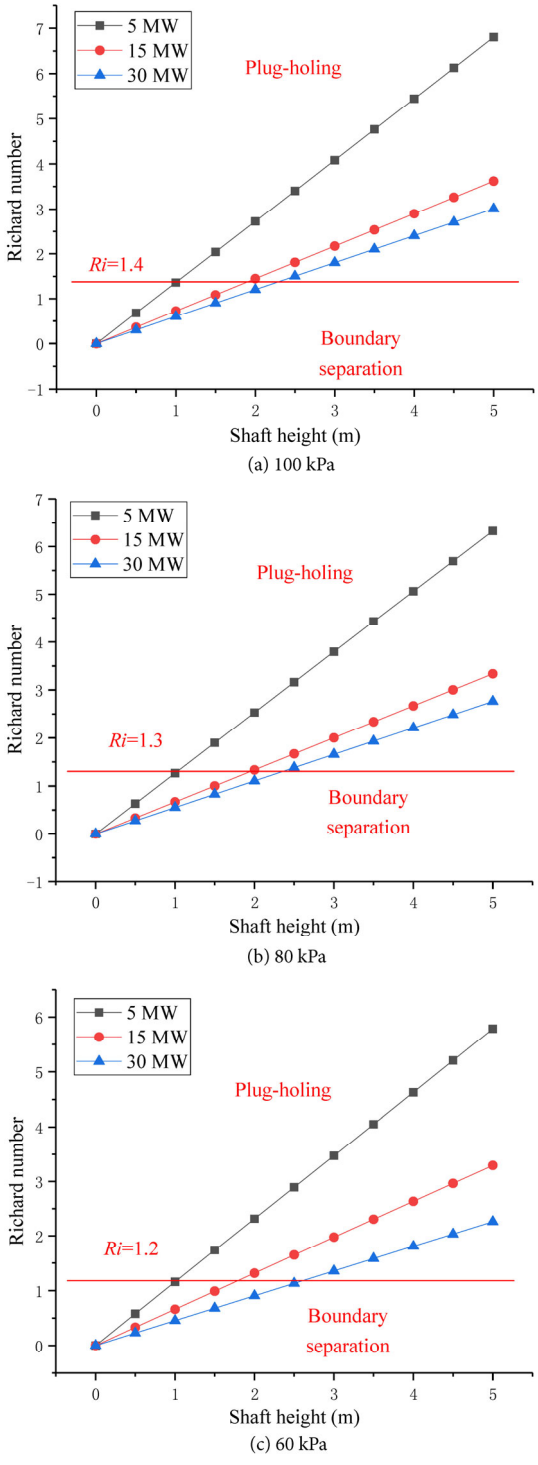

Fig. 10 Richard number under various ambient pressures and HRRs

5 Conclusions

First, a theoretical analysis is carried out to investigate the effects of ambient pressure on smoke velocity in the shaft since smoke temperature could be higher under lower ambient pressure due to lower heat loss and is the most important factor influencing smoke velocity. We conclude that smoke moves faster under lower ambient pressure.

To explore the effects of ambient pressure on the smoke movement pattern in shafts in a tunnel fire, a series of numerical simulations were conducted with varying ambient pressures, shaft heights and HRRs. The longitudinal smoke temperature under the shaft was used to distinguish the smoke movement pattern. The Richard number was adopted to determine the critical shaft height. We find that critical *Ri* decreases under reduced ambient pressure because the smoke velocity is higher under reduced ambient pressure due to higher smoke temperature, which is caused by lower heat loss.

Acknowledgements

This work was supported by the Funds of China Railway Corporation Science and Technology Development Program (No. P2018G007 and No. K2018G012), Sichuan Province Science and Technology Support Programs (No. 2018JY0566 and No. 2018RZ0109) and Tibet Research and Development Program (No. XZ201801-GB-07). The authors gratefully appreciate all these supports.

References

Alarie Y (2002). Toxicity of fire smoke. *Critical Reviews in Toxicology*, 32: 259–289.

Baek D, Bae S, Ryou HS (2017a). A numerical study on the effect of the hydraulic diameter of tunnels on the plug-holing phenomena in shallow underground tunnels. *Journal of Mechanical Science and Technology*, 31: 2331–2338.

Baek D, Sung KH, Ryou HS (2017b). Experimental study on the effect of heat release rate and aspect ratio of tunnel on the plug-holing phenomena in shallow underground tunnels. *International Journal of Heat and Mass Transfer*, 113: 1135–1141.

Cong HY, Wang XS, Zhu P, Jiang TH, Shi XJ (2017). Improvement in smoke extraction efficiency by natural ventilation through a board-coupled shaft during tunnel fires. *Applied Thermal Engineering*, 118: 127–137.

Cooper LY, Harkleroad M, Quintiere J, Rinkinen W (1982). An experimental study of upper hot layer stratification in full-scale multiroom fire scenarios. *Journal of Heat Transfer*, 104: 741–749.

Fan C, Ji J, Gao Z, Han J, Sun J (2013). Experimental study of air entrainment mode with natural ventilation using shafts in road tunnel fires. *International Journal of Heat and Mass Transfer*, 56: 750-757.

Fan C, Jin Z, Zhang J, Zhu H (2017). Effects of ambient wind on thermal smoke exhaust from a shaft in tunnels with natural ventilation. *Applied Thermal Engineering*, 117: 254–262.

Fan C, Chen J, Zhou Y, Liu X (2018a). Effects of fire location on the capacity of smoke exhaust from natural ventilation shafts in urban tunnels. *Fire and Materials*, 42: 974–984.

Fan C, Zhang L, Jiao S, Yang Z, Li M, Liu X (2018b). Smoke spread characteristics inside a tunnel with natural ventilation under a strong environmental wind. *Tunnelling and Underground Space Technology*, 82: 99–110.

Gong L, Jiang L, Li S, Shen N, Zhang Y, Sun J (2016). Theoretical and experimental study on longitudinal smoke temperature distribution in tunnel fires. *International Journal of Thermal Sciences*, 102: 319–328.

Guo Q, Zhu H, Yan Z, Zhang Y, Zhang Y, Huang T (2019). Experimental studies on the gas temperature and smoke back-layering length of fires in a shallow urban road tunnel with large cross-sectional vertical shafts. *Tunnelling and Underground Space Technology*, 83: 565–576.

Harish R, Venkatasubbaiah K (2014). Effects of buoyancy induced roof ventilation systems for smoke removal in tunnel fires. *Tunnelling and Underground Space Technology*, 42: 195–205.

He Y, Fernando A, Luo M (1998). Determination of interface height from measured parameter profile in enclosure fire experiment. *Fire Safety Journal*, 31: 19–38.

He S, Liang B, Pan G, Wang F, Cui L (2017). Influence of dynamic highway tunnel lighting environment on driving safety based on eye movement parameters of the driver. *Tunnelling and Underground Space Technology*, 67: 52–60.

He L, Xu Z, Chen H, Liu Q, Wang Y, Zhou Y (2018). Analysis of entrainment phenomenon near mechanical exhaust vent and a prediction model for smoke temperature in tunnel fire. *Tunnelling and Underground Space Technology*, 80: 143–150.

Hurley MJ (1995). SFPE Handbook Fire Protection Engineering. New York: Society of Fire Protection Engineers.

Ji J, Li K, Zhong W, Huo R (2010). Experimental investigation on influence of smoke venting velocity and vent height on mechanical smoke exhaust efficiency. *Journal of Hazardous Materials*, 177: 209–215.

Ji J, Gao ZH, Fan CG, Zhong W, Sun JH (2012). A study of the effect of plug-holing and boundary layer separation on natural ventilation with vertical shaft in urban road tunnel fires. *International Journal of Heat and Mass Transfer*, 55: 6032–6041.

Ji J, Han JY, Fan CG, Gao ZH, Sun JH (2013). Influence of cross-sectional area and aspect ratio of shaft on natural ventilation in urban road tunnel. *International Journal of Heat and Mass Transfer*, 67: 420–431.

Ji J, Fan C, Gao Z, Sun J (2014). Effects of vertical shaft geometry on natural ventilation in urban road tunnel fires. *Journal of Civil Engineering and Management*, 20: 466–476.

Ji J, Bi Y, Venkatasubbaiah K, Li K (2016). Influence of aspect ratio of tunnel on smoke temperature distribution under ceiling in near field of fire source. *Applied Thermal Engineering*, 106: 1094–1102.

Ji J, Guo F, Gao Z, Zhu J, Sun J (2017). Numerical investigation on the effect of ambient pressure on smoke movement and temperature distribution in tunnel fires. *Applied Thermal Engineering*, 118: 663–669.

Ji J, Guo F, Gao Z, Zhu J (2018). Effects of ambient pressure on transport characteristics of thermal-driven smoke flow in a tunnel. *International Journal of Thermal Sciences*, 125: 210–217.

Jiang X, Liao X, Chen S, Wang J, Zhang S (2018). An experimental study on plug-holing in tunnel fire with central smoke extraction. *Applied Thermal Engineering*, 138: 840–848.

Kashef A, Yuan Z, Lei B (2013). Ceiling temperature distribution and smoke diffusion in tunnel fires with natural ventilation. *Fire Safety Journal*, 62: 249–255.

Kim MB, Han YS, Yoon MO (1998). Laser-assisted visualization and measurement of corridor smoke spread. *Fire Safety Journal*, 31: 239–251.

Li A, Gao X, Ren T (2017). Study on thermal pressure in a sloping underground tunnel under natural ventilation. *Energy and Buildings*, 147: 200–209.

Liu C, Zhong M, Tian X, Zhang P, Xiao Y, Mei Q (2019). Experimental and numerical study on fire-induced smoke temperature in connected area of metro tunnel under natural ventilation. *International Journal of Thermal Sciences*, 138: 84–97.

McGrattan KB, Forney GP (2017). Fire Dynamics Simulator, User's Guide. New York: NIST Special Publication.

Meng F, He B, Zhu J, Zhao D, Darko A, Zhao Z (2018). Sensitivity analysis of wind pressure coefficients on CAARC standard tall buildings in CFD simulations. *Journal of Building Engineering*, 16: 146–158.

Mou B, He B, Zhao D, Chau KW (2017). Numerical simulation of the effects of building dimensional variation on wind pressure distribution. *Engineering Applications of Computational Fluid Mechanics*, 11: 293–309.

Oka Y, Oka H, Imazeki O (2016). Ceiling-jet thickness and vertical distribution along flat-ceilinged horizontal tunnel with natural ventilation. *Tunnelling and Underground Space Technology*, 53: 68–77.

Takeuchi S, Aoki T, Tanaka F, Moinuddin KAM (2017). Modeling for predicting the temperature distribution of smoke during a fire in an underground road tunnel with vertical shafts. *Fire Safety Journal*, 91: 312–319.

Takeuchi S, Tanaka F, Yoshida K, Moinuddin KAM (2018). Effects of scale ratio and aspect ratio in predicting the longitudinal smoke-temperature distribution during a fire in a road tunnel with vertical shafts. *Tunnelling and Underground Space Technology*, 80: 78–91.

Tanaka F, Kawabata N, Ura F (2016). Effects of a transverse external wind on natural ventilation during fires in shallow urban road tunnels with roof openings. *Fire Safety Journal*, 79: 20–36.

Tanaka F, Kawabata N, Ura F (2017). Smoke spreading characteristics during a fire in a shallow urban road tunnel with roof openings under a longitudinal external wind blowing. *Fire Safety Journal*, 90: 156–168.

Tang F, Hu LH, Yang LZ, Qiu ZW, Zhang XC (2014). Longitudinal distributions of CO concentration and temperature in buoyant tunnel fire smoke flow in a reduced pressure atmosphere with lower air entrainment at high altitude. *International Journal of Heat and Mass Transfer*, 75: 130–134.

Wan H, Gao Z, Han J, Ji J, Ye M, Zhang Y (2019). A numerical study on smoke back-layering length and inlet air velocity of fires in an inclined tunnel under natural ventilation with a vertical shaft. *International Journal of Thermal Sciences*, 138: 293–303.

Wang Y, Jiang J, Zhu D (2009). Diesel oil pool fire characteristic under natural ventilation conditions in tunnels with roof openings. *Journal of Hazardous Materials*, 166: 469–477.

Wang Y, Li Y, Yan P, Zhang B, Jiang J, Zhang L (2015). Maximum temperature of smoke beneath ceiling in tunnel fire with vertical shafts. *Tunnelling and Underground Space Technology*, 50: 189–198.

Wang Y, Sun X, Liu S, Yan P, Qin T, Zhang B (2016a). Simulation of back-layering length in tunnel fire with vertical shafts. *Applied Thermal Engineering*, 109: 344–350.

Wang Y, Yan P, Zhang B, Jiang J (2016b). Thermal buoyant smoke back-layering length in a naturally ventilated tunnel with vertical shafts. *Applied Thermal Engineering*, 93: 947–957.

Wang M, Yan G, Yu L, Xie W, Dai Y (2019). Effects of different artificial oxygen-supply systems on migrants' physical and psychological reactions in high-altitude tunnel construction. *Building and Environment*, 149: 458–467.

Xie B, Han Y, Huang H, Chen L, Zhou Y, Fan C, Liu X (2018). Numerical study of natural ventilation in urban shallow tunnels: Impact of shaft cross section. *Sustainable Cities and Society*, 42: 521–537.

Yan Z, Guo Q, Zhu H (2017). Full-scale experiments on fire characteristics of road tunnel at high altitude. *Tunnelling and Underground Space Technology*, 66: 134–146.

Yan G, Wang M, Yu L, Tian Y, Guo X (2020). Study of smoke movement characteristics in tunnel fires in high-altitude areas. *Fire and Materials*, 44: 65–75.

Yang D, Hu LH, Huo R, Jiang YQ, Liu S, Tang F (2010). Experimental study on buoyant flow stratification induced by a fire in a horizontal channel. *Applied Thermal Engineering*, 30: 872–878.

Yao Y, Cheng X, Zhang S, Zhu K, Shi L, Zhang H (2016). Smoke back-layering flow length in longitudinal ventilated tunnel fires with vertical shaft in the upstream. *Applied Thermal Engineering*, 107: 738–746.

Yao Y, Li Y, Ingason H, Cheng X (2019a). Numerical study on overall smoke control using naturally ventilated shafts during fires in a road tunnel. *International Journal of Thermal Sciences*, 140: 491–504.

Yao Y, Zhang S, Shi L, Cheng X (2019b). Effects of shaft inclination angle on the capacity of smoke exhaust under tunnel fire. *Indoor and Built Environment*, 28: 77–87.

Yuan Z, Lei B, Kashef A (2015). Experimental and theoretical study for tunnel fires with natural ventilation. *Fire Technology*, 51: 691–706.

Zhang S, He K, Yao Y, Peng M, Yang H, Wang J, Cheng X (2018). Investigation on the critical shaft height of plug-holing in the natural ventilated tunnel fire. *International Journal of Thermal Sciences*, 132: 517–533.

Zhao D, He B (2017). Effects of architectural shapes on surface wind pressure distribution: Case studies of oval-shaped tall buildings. *Journal of Building Engineering*, 12: 219–228.

Zhao S, Li Y, Ingason H, Liu F (2019). A theoretical and experimental study on the buoyancy-driven smoke flow in a tunnel with vertical shafts. *International Journal of Thermal Sciences*, 141: 33–46.

Zhong W, Fan CG, Ji J, Yang JP (2013). Influence of longitudinal wind on natural ventilation with vertical shaft in a road tunnel fire. *International Journal of Heat and Mass Transfer*, 57: 671–678.

Zhong M, Shi C, He L, Shi J, Liu C, Tian X (2016). Smoke development in full-scale sloped long and large curved tunnel fires under natural ventilation. *Applied Thermal Engineering*, 108: 857–865.

Zhou Y, Yang Y, Jiao S, Zhang L, Fan C, Ding C, Liu X (2019). Large Eddy Simulation of effectiveness of solid screen on improving natural ventilation performance in urban tunnels. *Tunnelling and Underground Space Technology*, 86: 174–185.

Zhu P, Tong X, Chen L, Wang C, Song H, Li X (2015). Influence of opening area ratio on natural ventilation in City tunnel under block transportation. *Sustainable Cities and Society*, 19: 144–150.